Enhancing the Efficiency of the Intermediate Band Solar Cells by Introducing: Carrier Losses, Alloying and Strain

Qiao-Yi Wang*, Judy Rorison

Photonics Group, University of Bristol, Bristol, BS8 1TR, UK

*Qiaoyi.wang@bristol.ac.uk

Abstract: A detailed balance model is used with a blackbody radiation function to determine the efficiency of an intermediate band solar cell including carrier losses from the intermediate band. The effect of the energy gap of the host semiconductor is examined as a function of the intermediate band position in the energy gap and the host semiconductor energy gap. Generally the optimum intermediate band level is found to decrease within the energy gap to mitigate the carrier losses and it is found that carrier losses are less detrimental to small energy gap materials. We therefore focus the study on the role of carrier losses in wide bandgap semiconductor intermediate band solar cell systems such as the GaN semiconductor with an Mn impurity band. Experimentally the Mn acceptor level in the GaN energy gap is found to be 1.8 eV above the valence band which is 199 meV off the ideal IB neglecting losses which reduces the efficiency to 21.36%. We demonstrate how carrier losses can be introduced into the system to shift the optimum IB position. Introducing carrier losses of 70% from the intermediate band, shifts the optimum intermediate band position to 1.8 eV above the valence band and increases the efficiency to 23.41%. We compare this to the effect of alloying the GaN and introducing biaxial strain to shift the effective position of the Mn impurity band within the bandgap to increase the efficiency.

1. Introduction

Intermediate Band Solar Cells (IBSCs) were proposed [1] as a variation of a compound III-V semiconductor p-i-n junction solar cell with a calculated maximum efficiency of 63% with maximum concentration of light [2] - making them the highest efficiency p-i-n junction solar cell possible. A schematic energy band profile of a p-i-n junction IBSC is given in Fig 1. A Detailed Balance Approach (DBA) introduced by Shockley and Queisser (SQ) [3] has been implemented to calculate the high efficiency proposed of 63% for a bandgap of 1.95 eV with the IB positioned 0.71 eV above the Valence Band (VB) or below the Conduction Band (CB). This approach produces an efficiency for a specific energy band gap and predicts the ideal position of the IB within

the bandgap as shown in Fig 2. The efficiency can be calculated when the IB is off the ideal position as it is found to decrease rapidly when the IB is off the ideal position.

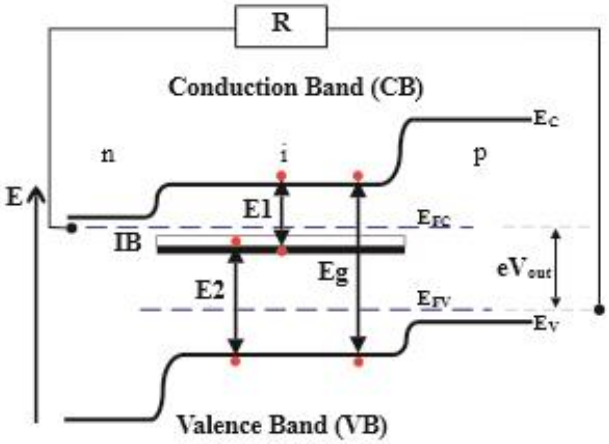

Fig. 1. *Schematic diagram of the energy band gap of intermediate band solar cell in p-i-n diode, and 3 possible optical absorption and emission processes with the associated photon energy Eg, E1 and E2.*

There are several possible approaches to create the Intermediate Band (IB): high density quantum dots of a smaller band gap material can be introduced into a larger bandgap semiconductor; or high density impurity states can also be introduced into the semiconductor host material to create an IB. Experimental efficiencies of around 15% have been observed for such devices employing QD-based IBs. The InAs/GaAs QD-IB

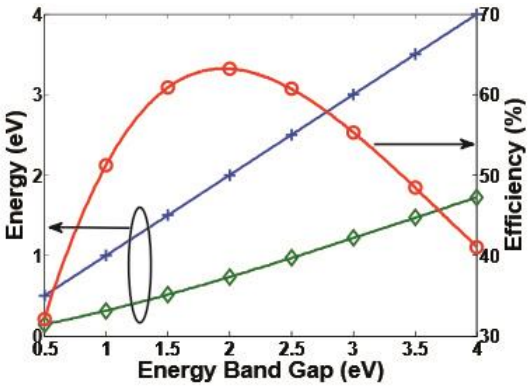

Fig. 2. *Maximum efficiency of the intermediate band solar cell is (red '○') as a function of the energy bandgap Eg (blue '+') for the optimum intermediate band position (green '◊'). The Eg line is plotted as a reference to compare with the intermediate band positions. The reference zero energy of the 'Energy'- axis could be either conduction band (Eg line represents valence band) or valance band (Eg line represents conduction band) in the ideal IBSC model.*

concentrator solar cell module are achieving efficiency of around 15.3% under 116 suns [4], which is still far below the predicted values.

We have previously examined the role of disorder in the energy levels of the states comprising the IB [2]. In this paper we propose to examine the role of carrier losses in affecting the efficiency. If the carrier losses occur from the CB or VB the total efficiency is reduced but the general shape of the efficiency as a function of the bandgap and the ideal position of the IB is unchanged. If the carrier loss is from the IB the balance of the generation and recombination of the VB↔IB and IB↔CB processes are affected and generation of more carriers from the VB→IB process is required to balance the carrier losses from the IB. The interplay of the absorption and the photon flux is important if the IB position is closer to the CB (E2<E1) or VB (E1<E2). If the losses from the IB are included, the optimum position of the IB is changed from that shown in Fig. 2. We present the results for the efficiency as a function of the energy bandgap. We find that the position of the IB is increased from the VB when losses from the IB are included as this increases the absorption range for the process EV→EIB. We observe that the loss of efficiency is more pronounced when the total energy gap is larger and also when the ideal IB position is closer to the VB.

It is important to engineer the correct IB position as the efficiency of the IBSC falls off sharply as the IB is moved from the ideal position. The introduction of controlled carrier losses (proton implantation, low temperature growth, etc.) may be a way to tune the IB position from the ideal (no losses) to that of a realistic systems which can offer improved efficiency as we demonstrate for the wide bandgap GaN system with a Mn impurity band. We also investigate how alloying and biaxial strain effects can be used to shift the VB and CB band edges and thereby effectively tune the IB position within the bandgap.

2. Theoretical model, results and analysis

2.1. IBSC ideal model

The IBSC ideal model is based on the SQ detailed balance method [1] and several

assumptions are made for the ideal model: 1) only the intrinsic photon absorption and spontaneous recombination processes are included. 2) In the ideal model the carrier mobility is taken to be infinite meaning that carriers contribute to the current if they are generated within the CB so carrier losses are neglected. 3) All three band gaps absorption profile are assumed to response for a continuous non-overlapping energy range. 4) Each absorbed photon generates an electron-hole pair. 5) In addition the cell is assumed thick enough to ensure total absorption of all the incident photons. 6) In the ideal model the IB is simulated as a single energy level instead of a narrow energy band requiring the excitation of an electron from the VB into the IB to be matched by excitation of this electron from the IB to the CB. Therefore, two electron rate equations for the IBSC should be involved:

$$\frac{dn_{CB}}{dt} = N_{gen\_cv} + N_{gen\_ci} - N_{rad_{cv}} - N_{rad_{ci}} - J/q \tag{1}$$

$$\frac{dn_{IB}}{dt} = N_{gen\_iv} + N_{rad\_ci} - N_{gen\_ci} - N_{rad\_iv} \tag{2}$$

Where $\frac{dn_{CB}}{dt}$ is the electron density change rate in CB and $\frac{dn_{IB}}{dt}$ is the electron density change rate in IB. N_{gen} is the photon absorption rate and one electron is generated by absorbing one photon. N_{rad} is the radiative recombination rate and only radiative recombination rate is involved due to the ideal IBSC model assumption (1). The suffixes indicate the band gap over which the generation happens.

This model focuses on the carrier population in the IB. As stated above the number of electrons in the IB is constant due to the balance of electrons entering from the VB and leaving to the CB. Therefore, the electron density variation rate in the time domain in the IB is zero at steady state, $\frac{dn_{CB}}{dt} = \frac{dn_{IB}}{dt} = 0$, thus the Eq. (2) can be reformed as

$$N_{gen\_iv} - N_{rad\_iv} = N_{gen\_ci} - N_{rad\_ci} \tag{3}$$

Any electrons promoted to the CB contribute to the current. Therefore, the current density 'J' is equal to the carrier density 'N' multiplied by the electron charge 'q'.

$$\frac{J}{q} = \left(N_{gen\_ci} - N_{rad\_ci}\right) + \left(N_{gen\_cv} - N_{rad\_cv}\right) \quad (4)$$

Due to the ideal IBSC model assumption (4), the electron density can be represented by a photon flux density function from the sun arriving at the solar cell and this is given as:

$$\mathrm{N}_i(\varepsilon_m, \varepsilon_M, \mu, T) = \mathrm{F_e}\left(\frac{2}{\mathrm{h^3c^2}}\right)\int_{\varepsilon_m}^{\varepsilon_M} \frac{\varepsilon^2 \mathrm{d}\varepsilon}{\mathrm{e}^{(\varepsilon-\mu)/\mathrm{k}T}-1} \quad (5)$$

Where the subscript i refers to the 3 possible transitions within the bandgap E1, E2 or Eg. And μ is chemical potential which is equivalent to the energy difference between quasi-Fermi levels, T is the temperature of the radiative body, the temperature for sun and solar cell are 6000K and 300K respectively. ε_m is the minimum absorption energy allowed, and ε_M is the maximum allowed in the non-overlapped band approximation. Fe is the geometric factor calculated as $\mathrm{F_e} = \mathrm{X} \cdot \mathrm{F_s}$, where Fs is the solid angle of photon flux of the Sun as seen from earth, which is around $2.16 \times 10^{-5}\pi$ and X is the concentrator factor which ranges from 1 to 46050.

The effect of the difference in refractive index between the air and the solar cell material on the isotropic radiation can be included in the Blackbody Radiation (BBR) for the solar cell emitting to ambient surrounding:

$$\mathrm{N}_i(\varepsilon_m, \varepsilon_M, \mu, T) = \mathrm{F_e}\left(\frac{2\mathrm{n_s^2}}{\mathrm{h^3c^2}}\right)\int_{\varepsilon_m}^{\varepsilon_M} \frac{\varepsilon^2 \mathrm{d}\varepsilon}{\mathrm{e}^{(\varepsilon-\mu)/\mathrm{k}T}-1} \quad (6)$$

Where n_s or n_0 is the refractive index of the solar cell material or air. h is Planck's constant, k is Boltzmann's constant, and c is the speed of light in vacuum respectively. And also $\mathrm{F_e} = \pi * \sin^2\theta_\mathrm{c} = \pi(\mathrm{n_0^2}/\mathrm{n_s^2})$. Snell's law states that θ_c is the critical angle which light can emit from a high refractive index material to a low refractive index material. And $\mu_{\mathrm{IV}} = \mathrm{E_{FI}} - \mathrm{E_{FV}}$; $\mu_{\mathrm{CI}} = \mathrm{E_{FC}} - \mathrm{E_{FI}}$ and $\mathrm{qV} = \mu_{\mathrm{CV}} = \mathrm{E_{FC}} - \mathrm{E_{FV}}$ as shown in Fig. 1.

From Eq. (3), μ_{CI} or μ_{IV} can be calculated as a function of voltage. Then it is substituted into Eq. (4), a relationship between current density 'J' and voltage 'V' can

be found. Afterwards, the output power density is P =V*J, which has a maximum point mathematically when $\partial P/\partial V = 0$. At the same time, we can work out the ideal IB position for specific bandgap by comparing the maximum output power of different IB positions. The detailed mathematical analysis can be found in our previous paper [2]. Meanwhile, the total energy density shining on the solar cells per unit area in unit time from the BBR of the Sun is,

$$P_{sun} = \mathrm{X} \cdot \mathrm{F}_s \left(\frac{2}{\mathrm{h}^3\mathrm{c}^2}\right) \int_0^\infty \frac{\varepsilon^3 \mathrm{d}\varepsilon}{\mathrm{e}^{\varepsilon/\mathrm{k}_B T_s - 1}} \tag{7}$$

Where Eq. (7) includes concentration factor 'X' and the solid angle of the Sun 'F_s'. Then, the maximum efficiency can be worked out by dividing maximum output power '$J_m V_m$' by power from the Sun 'P_{sun}' as:

$$\eta = \frac{J_m V_m}{P_{sun}} \tag{8}$$

2.2. Carrier losses

There are three different types of carrier losses: recombination from impurities or defects, also known as Shockley-Reed-Hall recombination (SRH), in the crystal structure (avoidable), spontaneous emission and Auger recombination (unavoidable). The spontaneous emission (also known as radiative recombination) is already included in the ideal model and result is shown in Fig. 2. The defect recombination is one of the

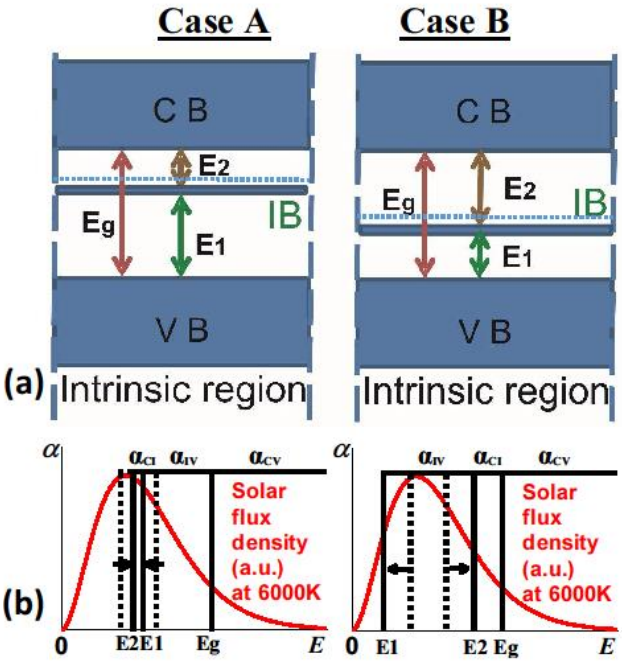

Fig. 3. *Two different situations in the intrinsic region of IBSC pin junction:*

a. Case A (top-left), IB is closer to CB; Case B (top-right), IB is closer to VB.

b. Their range of energies of the absorption spectra for each transition (bottom).

non-radiative recombination processes. The electrons annihilate so that there is always a negative sign in front of the rate, regardless of the band that it happens in. The Auger recombination may occur in three different types: CCCH, CHHS and CHHL, in which the Auger recombination rate could have a different sign in different circumstance in both bands. The defect recombination and Auger recombination were combined as the loss term in our loss model. And since there is either one carrier or three carriers involved in SRH or Auger recombination respectively, SRH is important for low carrier density which means it is not important for concentrator solar cells, meanwhile Auger recombination is important for high carrier density.

We add a carrier loss term in CB and VB as percentages c% and v% and also in the IB as an 'x' factor of net carrier population which is determined by generation minus spontaneous recombination combined with photon absorption rate for the transitions in Fig. 1. The carrier loss from CB or VB reduces the overall carriers by c% or v% from contribution to current as an expectable result in our model. Therefore, the investigation was carried out for the effect of loss in IB only. Therefore, Eq. (3) can be reformed as:

$$(1-x)\left(N_{gen\_iv}-N_{rad\_iv}\right)=N_{gen\_ci}-N_{rad\_ci} \tag{9}$$

Firstly, two situations should be introduced for the IBSC loss model, IB is closer to CB (Case A) and IB is closer to VB (Case B) as shown in Fig. 3. And the BBR function was used for photon absorption rate and radiative recombination rate. Without inducing loss carriers, the efficiency and IB position for the ideal cases without loss shown in Fig. 2, are the same for Case A and Case B in Fig. 3. By adding the loss term, the two cases have differing results as shown in Fig. 4.

From Fig. 4, there are five lines representing the efficiencies of five different situations with different loss percentages from the IB, in Case A and Case B. However, there are only four lines representing the optimised IB position from VB, since the optimised IBs do not exist if the carriers in the IB are totally wasted instead of contributing to output current for the situation that the loss percentage (x=1). The

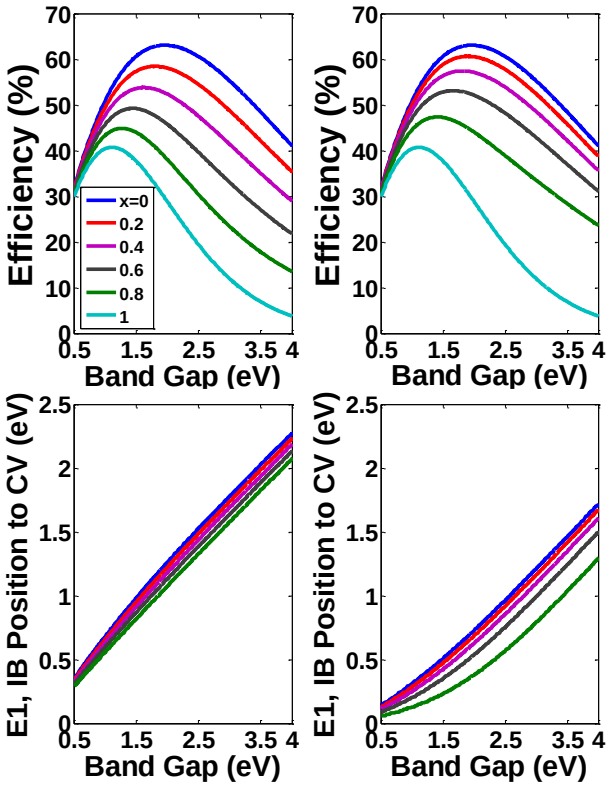

Fig. 4. *As x increases, Efficiency change as function of bandgap (top two) and the IB position from the conduction band change as function of bandgap (bottom two) for Case A (left) and Case B (right).*

situation (x=1) in each case indicates that only the bulk material absorption contributes to the overall current, in other words, no carrier can be excited and contributing to the current through the path VB→IB→CB. The general tendency is that the efficiency drops as the x factor increases, as expected since the loss term increases for the IB assisted electron pumping. And also, an important conclusion is that a lower IB position can lead to better efficiency under the same bandgap and x factor for both cases. This is an important conclusion which will be discussed in detail in next section. Now let us focus on the reason why the IB always moves towards the VB in both cases. As shown in two bottom absorption coefficient plots in Fig. 3, carrier population in IB is reduced as loss increases. Therefore, the net generation for the transition VB↔IB must be increased by shifting the IB position towards the VB which increases the integration range for the VB↔IB transition and also reduces the integration range for the IB↔CB transition from the equations as shown in (5) and (6). And since the shape of the solar spectrum is not uniformly distributed in the whole wavelength range, the shape leads

to the a curvature in the best IB position and efficiency in the loss model. In the Case B, two characteristics can be inferred:

- Larger IB position variation shows less efficiency reduction while increasing the loss in the IB, compared with Case A.
- E1 (IB to valence band) is the smallest bandgap, it wants to decrease more when it is located on the left side of solar spectrum peak.

However, Case A is much more closed to practical systems. Fig. 4 also depict that the carrier loss in the IB has less effect on efficiency in a low bandgap region than that in a large bandgap region. GaAs and GaN are two promising semiconductor representatives with a low bandgap and large bandgap respectively. They have around 1.42eV and 3.42eV direct bandgap at 300K. The large bandgap material GaN appears to be worth further investigations.

Here we introduce deep metallic impurity levels into the GaN system. Mn impurities doped in GaN (3.42eV bandgap) was reported to have an experimental result of a 1.8eV deep acceptor energy level above the valence band [5]. The original IB position in the non-loss model (Fig. 2) is 1.99eV above VB, with 49.57% efficiency. The efficiency from the original ideal IBSC model with 3.42eV bandgap and 1.8eV IB

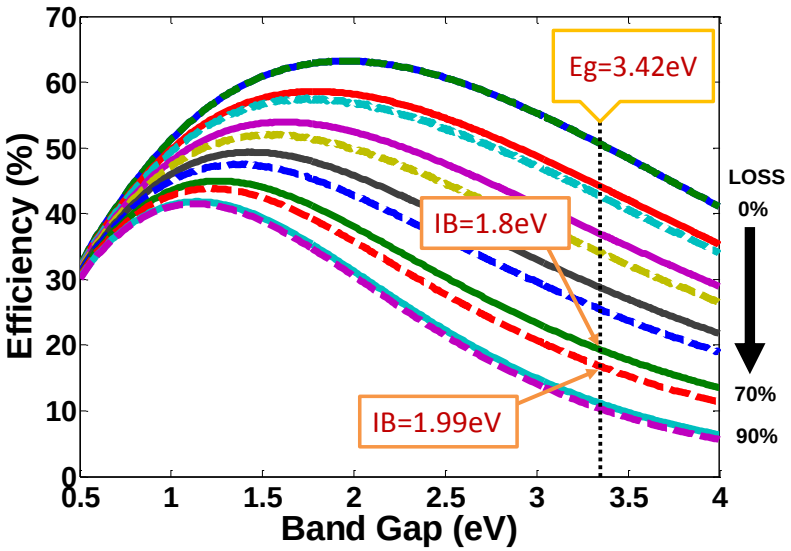

Fig. 5. *Loss model efficiency as function of bandgap, for original ideal IB position (dash lines) and the new shifted improved IB position (solid line). The x loss factor is labelled on the right hand side.*

position is 21.36% for Mn-doped GaN system. As depicted in Fig. 5, the new optimal

IB position is below the original ideal IB position to keep the detailed balance of population in the IB. Thus, the original IB gives a worse efficiency. It proves that my previous important conclusion from Fig. 4 that lower IB position can lead to better efficiency under the same bandgap and x factor, is established. And also, at the points where loss is equal to around 70% from IB for the GaN, original IB (1.99eV) gives 20.39% efficiency. Meanwhile, the new balanced IB position (1.8eV) gives 23.41% efficiency and this 1.8eV matches to the Mn impurities energy level in the GaN system.

2.3. Ternary Alloying

Apart from the carrier loss, we have also investigated moving the bandgap edges relative to the Mn level to try to bring it into the ideal IB position. Firstly we investigated alloying the GaN with In and secondly we investigated introducing biaxial strain effects. We investigate by alloying the GaN semiconductor with In to obtain $In_{1-X}Ga_XN$ assuming that a wurzite crystal structure is maintained for all compositions the bandgap Eg in units of eV can be tuned from 0.77eV (x=0) to 3.42eV (x=1) according to (3):

$$\mathrm{Eg} = 3.42x + 0.77(1-x) - 1.43x(1-x) \tag{10}$$

Since Mn is an impurity atom its energy is measured from the vacuum level depending on its electron affinity and is assumed to be independent of the host material. Then the position of the Mn energy level above the VB in $In_{1-X}Ga_XN$ alloy is E_{H_InGaN} and given as: [6]

$$\mathrm{E_{H\_InGaN}} = E_{H\_GaN} + \Delta E_G + \Delta\chi \tag{11}$$

Where $\Delta \mathrm{E_G}$ and $\Delta\chi$ are the bandgap value difference and the affinity value difference between the alloy $In_{1-X}Ga_XN$ and GaN.

2.4. Biaxial Strain

The Lattice Constant (LC) (α) is the length of the smallest unit cell edge and corresponds to the inter-atomic spacing. It can depend on crystal orientation, crystal structure and growth planes. When a crystal of a smaller (or larger) lattice constant is grown on a crystal of a larger (or smaller) atomic lattice constant biaxial-strain is introduced and acts to increase (or decrease) the atomic lattice constant introducing

tensile (or compressive) strain. The strain tensor, or lattice mismatch parameter can be defined as:

$$\boldsymbol{\varepsilon} \equiv \frac{\alpha_{native} - \alpha_{sub}}{\alpha_{native}} \tag{12}$$

Where α_{native} is the original unstrained lattice constant of native strained material, and α_{sub} is the lattice constant of substrate material. If $\alpha_{native} < \alpha_{sub}$ then the strain is tensile whereas if $\alpha_{native} > \alpha_{sub}$ then the strain is compressive. Pikus and Bir [7] derived the fundamental theory of bi-axial strain on cubic semiconductors and how the band edges are shifted and state degeneracy broken by a combination of hydrostatic H and shear S forces. This can be represented in an 8x8 interaction matrix including the CB, and the VB comprising the Heavy Hole (HH), Light Hole (LH) and Spin-Off (SO) bands. The resulting band edge levels of the CB (E_{CB-S}), HH (E_{HH-S}), LH (E_{LH-S}) and SO (E_{SO-S}) including strain (signified by the subscript 's') are [7]:

$$E_{CB-S} = E_{CB} + H_C \tag{13a}$$

$$E_{HH-S} = E_{VB} - (H_V - S) \tag{13b}$$

$$E_{LH-S} = E_{VB} - (H_V + S - \delta) \tag{13c}$$

$$E_{SO-S} = (E_{VB} - \Delta) - (H_V + \delta) \tag{13d}$$

Where E_{CB} and E_{VB} are CB and VB energy levels of unstrained system and the energies $H_{C,V}$ and S are referred to as the hydrostatic component and shear component of strain. And Δ is spin-orbit split off (SOSO) energy. δ represents an additional repulsion between the LH and SO bands. They are related to the strain tensor via the deformation potentials a and b[7]:

$$H_{C,V} = (-a_{c,v}) \cdot 2\frac{C_{11} - C_{12}}{C_{11}}\varepsilon \tag{14}$$

$$S = (-b) \cdot \frac{C_{11} + 2C_{12}}{C_{11}}\varepsilon \tag{15}$$

$$\delta = \frac{1}{2}\Delta\left\{[1 - 2(S/\Delta) + 9(S/\Delta)^2]^{1/2} - (1 - S/\Delta)\right\} \approx 2S^2/\Delta \tag{16}$$

Where the C_{11} and C_{12} are the elastic stiffness coefficients or elastic moduli (EM). The a_c and a_v are Hydrostatic Deformation Potentials (HDP) for CB and VB respectively. The b is Shear Deformation Potential (SDP). All the strain related parameters of GaN and InN are listed in Table 1. The parameters for $In_{1-X}Ga_XN$ are calculated with the formula: $x(\mathbf{GaN}) + (1-x)(\mathbf{InN})$. Where the (material) should be replaced by associated strain related values. Since the Mn impurity band level is not affected by the host material which was introduced in the last section, the strain is assumed to change the conduction band and three valence bands only.

Table 1 Material parameters for strain calculation of InGaN constituent binary alloys.[10]

	symbol	(units)	GaN	InN
LC	α	(Å)	4.5	4.98
HDP	a_c	(eV)	-2.2	-1.85
	a_v	(eV)	-5.2	-1.5
SDP	b	(eV)	-2.2	-1.2
EM	C_{11}	(GPa)	293	187
	C_{12}	(GPa)	159	125
SOSO	Δ	(eV)	0.02	0.003

Fig. 6a and Fig. 6b show the real and ideal efficiency of the $In_{1-X}Ga_XN$ system as a function of the composition assuming the composition is lattice-matched to the substrate (black lines) and Fig. 6a takes into account that the alloy is grown on a GaN substrate (red-line) which results in compressive strain that varies with composition. Fig. 6b considering that it is grown on an InN substrate (blue line) resulting in a tensile strain which varies with composition. The ideal IB (associated with the ideal efficiency) and the real Mn positions (associated with the real efficiency) are also shown.

In Fig. 6a, for the unstrained case at x=0.2, the real Mn position matches the ideal IB position and the real and ideal efficiencies match. This gives a maximum efficiency

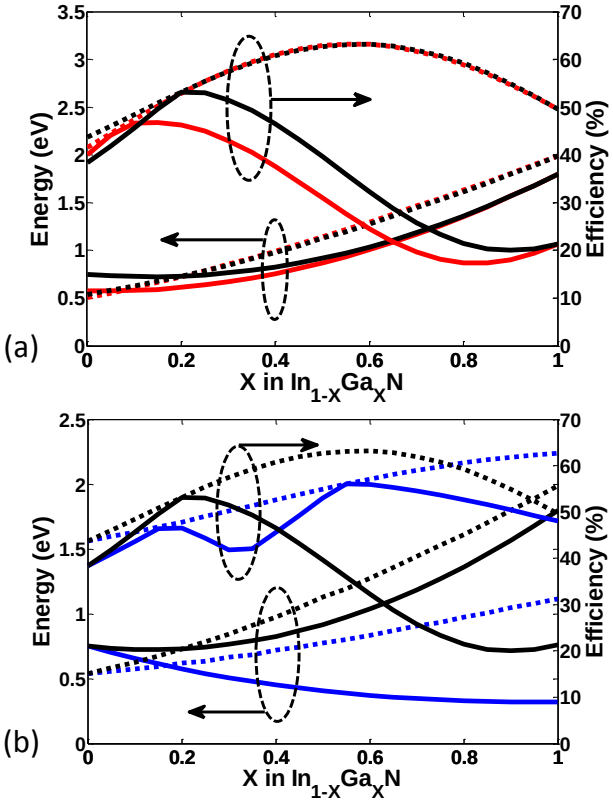

Fig. 6. *Efficiency (right-arrowed) of the Intermediate Band Solar Cells as a function of the $In_{1-x}Ga_xN$ composition considering the ideal (dotted) and real $Mn^{+3/2}$ (solid) intermediate band position (left-arrowed). (a) Unstrained $In_{1-x}Ga_xN$ system (Black) and compressively strained $In_{1-x}Ga_xN$/GaN system (Red); (b) Unstrained $In_{1-x}Ga_xN$ system (Black) and tensile strained $In_{1-x}Ga_xN$/InN system (Blue).*

of 53.17% for the real Mn in $In_{0.8}Ga_{0.2}N$. Including compressive strain shifts the matching position of the ideal and real IB position to x=0.1 resulting in a maximum efficiency of 46.6% which occurs for $In_{0.9}Ga_{0.1}N$ with a compressive strain of 8.76%. For Fig. 6b we see that strain has a large effect on the ideal and real IB positions, particularly as the strain is increased as x increases. We observe two crossings of the real and ideal IB positions at x=0.17 with efficiency of 47.10% and at x=0.55 with efficiency of 56.02%. This occurs because the IB position can be above the VB or below the CB. The tensile strained system $In_{0.45}Ga_{0.55}N$/InN (with -5.6% tensile strain) does offer an improvement in the efficiency of about 3% when compared with the unstrained case, however it is still far from the peak value of 63.27%. In the reality, the strain is responsible for the formation of dislocation, which limits the operating lifetime

of device. The biaxial strain up to 2% is roughly used in laser. Strain >3% would introduce defects. [9]

3. Conclusion

Firstly, we briefly introduced the theory of IBSC and presented the theoretical maximum efficiency of an ideal IBSC of around 63% at 1.95eV bandgap and 0.71eV IB position under the SQ detailed balanced method with the use of a blackbody radiation function. Then, we studied the characteristics of IBSC with loss term added in IB. We concluded that lower IB position can lead to better efficiency under the same bandgap and x factor. And also, the carrier loss in the IB has less effect on the efficiency in low bandgap region than in a large bandgap region. Therefore, we use Manganese (Mn) acceptors in the large bandgap material GaN, which has an acceptor level 1.8eV (above the VB) off the ideal IB position in the ideal model, and it reduced the efficiency greatly to 21.36%. We demonstrated how losses can be used to shift the ideal IB position. A 70% carrier loss from the IB and the ideal IB position shifted to 1.8eV for GaN systems increases the efficiency to 23.41%. It was found that the system is very sensitive to the position of the IB and that combining the ternary alloy InGaN and biaxial strain can be used to improve the IB position and therefore raise the efficiency of realistic IBSCs.

4. Acknowledgements

The authors acknowledge financial support from UK EPSRC under grant no. EP/K029665/1.

5. Reference

[1] A. Luque and A. Marti, “Increasing the efficiency of ideal solar cells by photon induced transitions at intermediate levels,” *Phys. Rev. Lett.*, vol. 78, no. 26, pp. 5014–5017, 1997.

[2] Q.-Y. Wang and J. Rorison, “Modelling of quantum dot intermediate band solar cells: effect of intermediate band linewidth broadening,” *IET Optoelectron.*, vol. 8, no. 2, pp. 81–87, Apr. 2014.

[3] W. Shockley and H. J. Queisser, “Detailed Balance Limit of Efficiency of p-n Junction Solar Cells,” *J. Appl. Phys.*, vol. 32, no. 3, pp. 510–519, 1961.

[4] Y. Okada, K. Yoshida, Y. Shoji, and T. Sogabe, “Recent progress on quantum dot intermediate band solar cells,” *IEICE Electron. Express*, vol. 10, no. 17, p. 20132007, 2013.

[5] T. Graf, M. Gjukic, M. S. Brandt, M. Stutzmann, and O. Ambacher, “The Mn(3+/2+) acceptor level in group III nitrides,” *Appl. Phys. Lett.*, vol. 81, no. 27, pp. 5159–5161, 2002.

[6] A. Martí, C. Tablero, E. Antolín, A. Luque, R. P. Campion, S. V Novikov, and C. T. Foxon, “Potential of Mn doped In1−xGaxN for implementing intermediate band solar cells,” *Sol. Energy Mater. Sol. Cells*, vol. 93, no. 5, pp. 641–644, May 2009.

[7] G. E. Pikus and G. L. Bir, “Effect of deformation on the hole energy spectrum of germanium and silicon,” *Sov. Physics-Solid State*, vol. 1, no. 11, pp. 1502–1517, 1960.

[8] L. A. Coldren and S. W. Corzine, *Diode lasers and Photonic Integrated Circuits*. John Wiley &sons, Inc., 1995.

[9] A. R. Adams, “Strained-layer quantum-well lasers,” *IEEE J. Sel. Top. Quantum Electron.*, vol. 17, no. 5, pp. 1364–1373, 2011.

[10] I. Vurgaftman, J. R. Meyer, and L. R. Ram-Mohan, “Band parameters for III–V compound semiconductors and their alloys,” *J. Appl. Phys.*, vol. 89, no. 11, pp. 5815–5875, 2001.